XLVI CILAMCE
VITÓRIA - ES - BRAZIL - 2025
XLVI IBERO-LATIN AMERICAN CONGRESS ON COMPUTATIONAL METHODS IN ENGENEERING

An optimized adaptive semi-explicit/explicit time-marching formulation for elastodynamic analyses

Caio A. Cavalcanti[1], Delfim Soares Jr.[2], Webe J. Mansur[1]

[1]*COPPE/Federal University of Rio de Janeiro*
CEP 21941-611, Rio de Janeiro, RJ, Brazil
caio.cavalcanti@coc.ufrj.br, webe@coc.ufrj.br
[2]*Structural Engineering Dept., Federal University of Juiz de Fora*
CEP 36036-330, Juiz de Fora, MG, Brazil
delfim.soares@ufjf.edu.br

Abstract. This work presents an optimized adaptive semi-explicit/explicit time integration strategy to analyse elastodynamic models. The discussed methodology is based on two time-integration parameters, which are allowed to assume different values for each element of the adopted spatial discretization. The computation of the first parameter is designed to improve accuracy and to ensure the stability of the analysis, and it defines the so-called semi-explicit and explicit elements of the model. The evaluation of the second parameter focuses on enabling an effective numerical dissipative algorithm, and it defines the so-called dissipative and non-dissipative elements of the model at each time step of the analysis. These adaptive time-integration parameters are computed taking into account the physical and geometrical properties of the elements, the adopted time-step value, and local previous time step results. The resulting formulation is very accurate and efficient. To improve the effectiveness of this technique, optimal time-step values are automatically evaluated, taking into account a particle swarm optimization algorithm, which allows to establish the most efficient distribution of semi-explicit and explicit elements along the model for solution. Numerical results are presented at the end of the paper, illustrating the good performance of the optimized hybrid approach.

Keywords: Time-integration, Hybrid formulation, Adaptive parameters, Optimized solution, Elastodynamics.

1 Introduction

Time-domain hyperbolic differential equations play a central role in various fields of science and engineering, particularly in problems involving wave propagation in solid media. Due to the complexity of the physical domains and boundary conditions involved, analytical solutions to such equations are often unattainable. In this context, numerical methods based on spatial and temporal discretization are employed to approximate the solution with adequate accuracy and computational efficiency.

Typically, spatial discretization is performed independently of the temporal discretization, using well-established techniques such as the finite element method, meshless methods etc. This leads to a semi-discrete system of ordinary differential equations in time, which must then be solved using a time integration algorithm. A wide range of both explicit and implicit integration schemes are available in the literature [1-5]. Explicit schemes are computationally efficient but conditionally stable, imposing limitations on the time step size. In contrast, implicit methods are generally unconditionally stable but involve higher computational cost per time step.

To combine the advantages of both schemes, hybrid time integration methodologies have been proposed [6-10]. These approaches rely on a local analysis of the geometric and physical properties of each element in the spatial discretization to classify them as either explicit or implicit, thereby ensuring global stability of the simulation regardless of the chosen time step. This property enables the formulation of an optimization problem aimed at determining the time step that minimizes the total number of operations. Previous studies by Soares et al.

[6,7] have shown that nature-inspired metaheuristic optimization algorithms, such as Particle Swarm Optimization (PSO), are effective in solving this problem without requiring an exhaustive search, even in the absence of a known objective function.

Another critical aspect of numerical integration methods is numerical damping [4-10]. When appropriately applied, algorithmic damping significantly enhances the accuracy of the adopted scheme by mitigating spatial discretization errors that are transferred to the resulting semi-discrete system, due to an inappropriate representation of high-frequency vibration modes. Therefore, an effective damping strategy should target only the highest natural frequencies of the model, preserving the physical behavior of the system.

This work presents the results obtained by applying the semi-explicit/explicit methodology developed by Soares [11] to linear elastodynamic models, in combination with a fully automatic procedure for optimizing the time step via the Particle Swarm Optimization (PSO) algorithm [12-14]. The methodology is defined by two locally evaluated parameters: the first ensures numerical stability, while the second introduces numerical damping according to the detection of local oscillations. The paper presents the computed responses for two distinct example models, along with the corresponding CPU times and relative errors whenever analytical response is available, to demonstrate the performance and efficiency of the proposed approach.

2 Governing equations and time solution strategy

The hyperbolic semi-discrete system of equations that governs the behaviour of a dynamic system is given by:

$$\mathbf{M}\ddot{\mathbf{U}}(t) + \mathbf{C}\dot{\mathbf{U}}(t) + \mathbf{K}\mathbf{U}(t) = \mathbf{F}(t)\,, \tag{1}$$

where **M**, **C** and **K** are, respectively, the mass, damping, and stiffness matrices obtained in this work via the Finite Element Method [15]. The vectors $\ddot{\mathbf{U}}(t)$, $\dot{\mathbf{U}}(t)$, $\mathbf{U}(t)$, and $\mathbf{F}(t)$ represent respectively the accelerations, velocities, displacements, and the nodal external forces at time instant *t*.

The time solution strategy described by Soares [11] comprises the use of two integration parameters evaluated locally at each element of the discretized model. Initially, eq. (1) may be expressed as function of the time step *n*, where $t^n = n\Delta t$, and Δt is the time step size of the analyses. Then, by applying an α parameter as in standard α-methods [4] (i.e., pondering the internal forces at the current and previous time steps), eq. (1) may be rewritten as:

$$\mathbf{M}\ddot{\mathbf{U}}^n + \mathbf{C}\dot{\mathbf{U}}^n + (1+\alpha)\mathbf{K}\mathbf{U}^n - \alpha\mathbf{K}\mathbf{U}^{n-1} = \mathbf{F}^n. \tag{2}$$

By considering the Central Difference Method approximations for the time derivatives of the displacements, and by writing eq. (2) for each element of the spatially discretized model (indicated by subscript *e*), the following solution algorithm takes place:

$$\left(\overline{\mathbf{M}}_e + \tfrac{1}{2}\Delta t\mathbf{C}_e\right)\mathbf{U}_e^{n+1} = \Delta t^2[\mathbf{F}_e^n - (1+\alpha_e^n)\mathbf{K}_e\mathbf{U}_e^n + \alpha_e^n\mathbf{K}_e\mathbf{U}_e^{n-1}] + \overline{\mathbf{M}}_e(2\mathbf{U}_e^n - \mathbf{U}_e^{n-1}) + \tfrac{1}{2}\Delta t\mathbf{C}_e\mathbf{U}_e^{n-1}, \tag{3}$$

where $\overline{\mathbf{M}}_e$ stands for a modified local mass matrix, which may be computed as:

$$\overline{\mathbf{M}}_e = \mathbf{M}_e + \Delta t^2 a_e\mathbf{K}_e\,, \tag{4}$$

where a_e is another integration parameter that makes it possible for the featured strategy to have guaranteed stability.

As one may observe, different spacial and temporal values may be considered for the above reported time integration parameters. Equations (3) and (4) show that, if lumped mass and damping matrices are regarded, a null a_e value produces a diagonal local effective matrix, resulting in an explicit element whose solution could be carried out without the need of a solver routine. Thus, the above discussed solution strategy may yield hybrid analyses (according to the a_e values that are applied to each element) considering reduced systems of equations due to the existence of explicit elements along the model, meaning that this technique may become more efficient than standard fully implicit algorithms. Additionally, this hybrid approach may be automatically established, requiring no extra effort or expertise from the user, once the a_e parameters are properly defined.

The computation of a_e is carried out based on the maximal sampling frequencies of each subdomain (Ω_e^{max}) as follows [11]:

$$\text{if } \Omega_e^{max} \leq 2, a_e = 0, \tag{5a}$$

$$\text{if } \Omega_e^{max} > 2, a_e = \frac{1}{4}\tanh\left(\frac{1}{4}\Omega_e^{max}\right). \tag{5b}$$

Taking into consideration the α parameter, it is locally applied only at elements where oscillations are verified at any of its degrees of freedom (η_e). Furthermore, its implementation does not necessarily occur at all time steps, but only at those where the referred vibrations are observed. This can be carried out via the computation of a local oscillatory parameter φ_e^{n+1} that takes into account the response of three consecutive time steps (u^{n-1}, u^n, and u^{n+1}) and computes the difference between the increment in the response within two consecutive time steps (i.e., $|u^{n+1} - u^{n-1}|$) and the sum of the corresponding increments within one time step (i.e., $|u^{n+1} - u^n| + |u^n - u^{n-1}|$). An oscillation occurs when this difference is not null, meaning that numerical dissipation will be applied at the current time step ($n + 1$). Also, numerical damping may only be applied after $m + 1$ consecutive oscillations are observed (it is recommended that $m = 0$ or $m = 1$ is adopted). Mathematically, this idea may be carried out as follows:

$$\varphi_e^{n+1} = \sum_{i=1}^{\eta_e}\left||u_i^{n+1} - u_i^{n-1}| - |u_i^{n+1} - u_i^n| - |u_i^n - u_i^{n-1}|\right|. \tag{6}$$

$$\text{If } \left(\bigcup_{j=n+1-m}^{n+1}\left(\varphi_e^j = 0\right)\right), \alpha_e^{n+1} = 0. \tag{7a}$$

$$\text{If } \left(\bigcup_{j=n+1-m}^{n+1}\left(\varphi_e^j \neq 0\right)\right), \alpha_e^{n+1} = \frac{2}{\Omega_e^{max}}\left[\left(1 + \xi_e\Omega_e^{max} + a_e\Omega_e^{max}\right)^{\frac{1}{2}} - \xi_e\right] - 1, \tag{7b}$$

where ξ_e is computed taking into consideration the physical properties of the element that define its mass and damping matrices, namely ρ_e and ς_e, respectively, and it is given by:

$$\xi_e = \varsigma_e \Delta t / 2\rho_e\Omega_e^{max}. \tag{8}$$

This hybrid integration scheme allows an optimal Δt to be searched in a specified range, i.e., a time step size that provides the least number of algorithmic operations. One possible search interval is that limited inferiorly by the largest Δt where all elements of the analysis are explicit, and superiorly by the smallest Δt where all the elements are non-explicit. Aiming at higher efficiency, instead of an exhaustive search, a meta-heuristic optimization algorithm may be employed to provide a good approximation for this optimal time step size without requiring high computational effort. In this study, the PSO algorithm is employed due to its good convergence rate in problems involving only one variable and the implementation simplicity associated with this optimization technique.

3 Numerical applications

In this section, two numerical case studies are presented to demonstrate the capabilities and performance of the proposed hybrid integration scheme. The first example addresses the axial motion of a point located at the interface between two distinct materials in a clamped rod. Two different configurations are considered, varying the physical properties of the constituent materials. This example allows for a direct assessment of the method's accuracy, as an analytical solution is available for comparison, developed in the work of Batra *et al.* [16].

The second case study involves a synthetic geophysical model characterized by a high degree of structural complexity, representative of real-world applications in the OIL & GAS industry, as presented by Fehler [17]. Although no analytical solution is available for this configuration, the example serves to highlight the method's effectiveness in handling large-scale, highly heterogeneous problems.

In all simulations, the semi-explicit/explicit integration technique is evaluated against standard time integration methods, including the explicit Central Difference Method (CDM) [3], the Trapezoidal Rule (TR) [3], and the implicit Generalized-α (IG-α) method [4]. For the discussed hybrid formulation and fully implicit schemes (i.e., TR and IG-α), the optimized Δt value that is computed to the hybrid approach is employed, as stability is inherently ensured by these techniques. Conversely, the CDM considers the use of its critical Δt value, due to its conditional stability. For the IG-α method, a spectral radius of ρ_∞= 0.5 is adopted, introducing "moderate" numerical damping into the response.

3.1 Application 1

This first example studies a heterogeneous rectangular rod that is subjected to a dynamic axial loading and is clamped at one of its ends, as illustrated in Fig. 1:

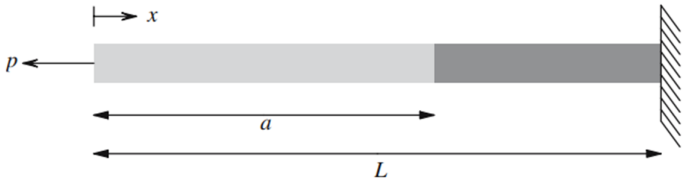
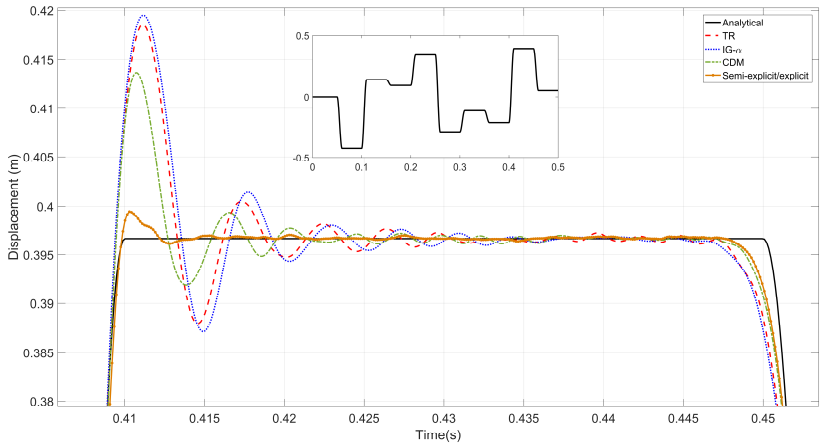


Figure 1. Sketch of the analysed model

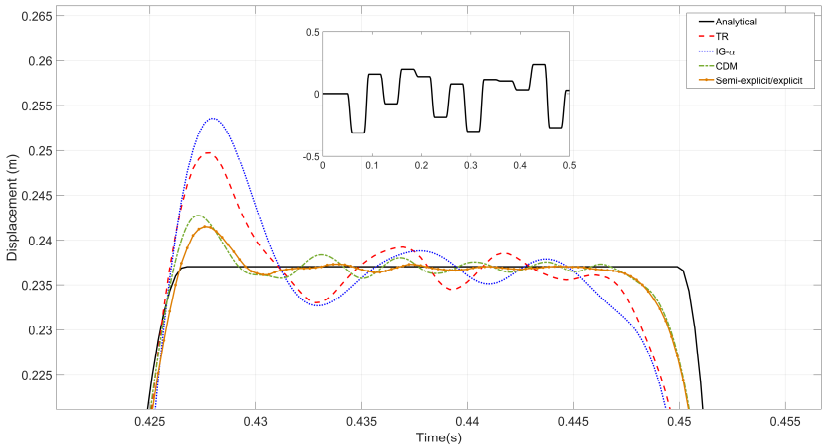
The external force is applied at the free end and varies over time according to the following expression:

$$p(t) = A \sin\left(\frac{\pi t}{T}\right)[H(t) - H(t-T)], \tag{9}$$

where A denotes the load amplitude, T represents the total duration of the applied loading, and $H(\cdot)$ is the Heaviside step function.



(a)



(b)

Figure 2. Time-history results for u_x, where: (a) $c_2/c_1 = 2$; (b) $c_2/c_1 = 3$

The total length of the rod is $L = 1m$, with the first region extending from $x = 0$ to $x = a$, where $a = L/2$. The remaining segment, from $x = a$ to $x = L$, constitutes the second region. Each region is composed of a distinct material. Both materials are assumed to have zero Poisson's ratio ($\nu_1 = \nu_2 = 0$), null damping ($\varsigma_1 = \varsigma_2 = 0$), and identical mass densities ($\rho_1 = \rho_2 = 1\ kg/m^3$). However, they differ in their elastic behavior, characterized by distinct moduli of elasticity. Two configurations are considered. In the first, the Young's moduli are given by $E_1 = 100\ N/m^2$ and $E_2 = 4E_1$, resulting in a dilatational wave speed in the second region twice that of the first ($c_2 = 2c_1$). In the second configuration, E_1 remains unchanged, while $E_2 = 9E_1$, leading to a dilatational wave speed three times greater in the second region ($c_2 = 3c_1$).

The obtained numerical results at the interface point $x = a$ are presented in Fig. 2 for both material configurations, considering a discretized model composed of 55,986 linear triangular elements. These time-history responses clearly demonstrate the better accuracy of the adaptive semi-explicit/explicit formulation when compared to the selected standard time integration schemes. Table 1 summarizes the time step sizes, relative errors, and CPU times for each method, where these CPU times represent the mean value computed over three consecutive runs for each configuration, providing a better representation for this amount. The computation of the described optimized time step sizes for the hybrid approach took, on average, 2% of the indicated total CPU time. Also, these computed time step sizes resulted in a percentage of 2.30% and 55.15% of non-explicit elements for the considered first and second models, respectively.

For both material configurations, the proposed hybrid scheme provides better accuracy than the CDM, despite employing significantly larger time steps. Furthermore, as the wave speed ratio c_2/c_1 increases, the performance of the CDM is notably affected, requiring smaller critical time steps to maintain stability. In contrast, methods with guaranteed stability – including the semi-explicit/explicit approach – remain unaffected by this limitation and sustain their computational efficiency.

Overall, these results demonstrate that the optimized hybrid strategy consistently outperforms conventional integration schemes in terms of accuracy and computational cost. This advantage may become even more pronounced for heterogeneous models with significant contrasts in material properties, highlighting the robustness and efficiency of the adaptive formulation for practical elastodynamic applications.

Table 1. Performance of the methods in the first application

c_2/c_1	Method	Δt (10^{-4}s)	Error (10^{-2})	CPU Time (s)
2	CDM	0.81716 (1.00)	0.98 (1.43)	53.70 (1.26)
	TR	1.35321 (1.66)	1.51 (2.21)	107.51 (2.53)
	IG-α		1.72 (2.51)	127.94 (3.01)
	Semi-explicit/explicit		0.69 (1.00)	42.56 (1.00)
3	CDM	0.54477 (1.00)	1.49 (1.01)	78.75 (1.84)
	TR	2.75511 (5.06)	4.15 (2.80)	51.56 (1.20)
	IG-α		5.32 (3.59)	61.16 (1.43)
	Semi-explicit/explicit		1.48 (1.00)	42.91 (1.00)

3.2 Application 2

To further assess the performance and applicability of the proposed semi-explicit/explicit integration scheme, a second numerical example is presented, focusing on a synthetic geophysical model representative of complex subsurface structures typically encountered in the OIL & GAS industry. This benchmark configuration simulates a heterogeneous geological domain with stratified layers and salt bodies, which impose significant challenges for elastodynamic wave propagation analyses [10, 17]. In this case, an impulsive vertical load is applied in the center-top region of the model. The discretized model has 717,319 linear triangular elements and 299 distinct materials, which are depicted by different colours in Fig. 3.

The PSO algorithm calculated an optimal time step size of 3.25509s, providing a total of 0.15% non-explicit elements in the analysed model, and it took 0.80% of the total CPU time. Table 2 summarizes the performance of each method, confirming the effectiveness of the semi-explicit/explicit scheme. Figure 4 shows the computed displacement modulus (in logarithmic scale) along the model, at three different time instants, for the hybrid approach and the CDM.

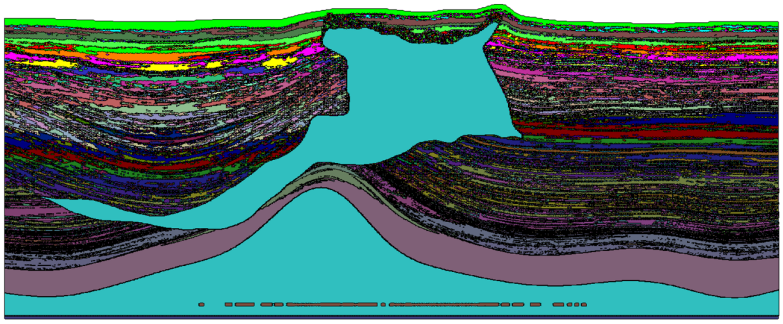


Figure 3. Considered geophysical model.

Table 2. Performance of the methods in the second application

Method	Δt (10^{-3}s)	CPU Time (s)
CDM	2.31651 (1.00)	300.26 (1.03)
TR	3.25509 (1.41)	3598.08 (12.32)
IG-α		3414.81 (11.69)
Semi-explicit/explicit		292.06 (1.00)

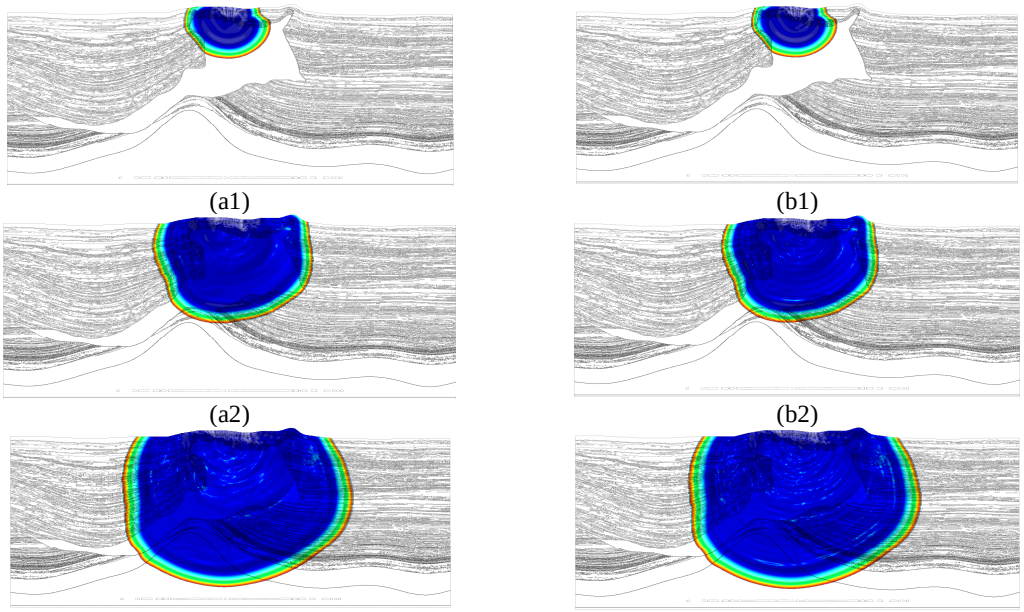


Figure 4. Time-history results for $\|\boldsymbol{u}\|$: (a) semi-explicit/explicit, (b) CDM; (1) 0.92s, (2) 1.84s, and (3) 2.76s

4 Conclusions

The presented numerical results indicate that the proposed semi-explicit/explicit time integration strategy effectively combines high accuracy with significant computational efficiency for elastodynamic analyses. The hybrid approach maintained stability with larger time steps and minimized spurious high-frequency oscillations through adaptive local damping, confirming its robustness for complex configurations.

The optimization routine consistently produced near-optimal time steps with negligible overhead, ensuring an efficient explicit/non-explicit element distribution without user intervention. Even in complex geophysical configurations, the method demonstrated performance comparable to fully explicit schemes while retaining the stability that is typical of implicit formulations.

These findings reinforce the potential of the discussed adaptive semi-explicit/explicit formulation as a practical alternative for large-scale dynamic simulations where accuracy, efficiency, and ease of implementation are equally required.

Acknowledgements. The financial support by CAPES (Coordenação de Aperfeiçoamento de Pessoal de Nível Superior), PETROBRAS, and FAPEMIG (Fundação de Amparo à Pesquisa do Estado de Minas Gerais) is greatly acknowledge.

Authorship statement. The authors hereby confirm that they are the sole liable persons responsible for the authorship of this work, and that all material that has been herein included as part of the present paper is either the property (and authorship) of the authors, or has the permission of the owners to be included here.

References

[1] G. Noh and K. J. Bathe, "An explicit time integration scheme for the analysis of wave propagations". *Computers & Structures*, vol. 129, pp. 178-193, 2013.
[2] K. J. Bathe and M. M. I. Baig, "On a composite implicit time integration procedure for nonlinear dynamics". *Computers & Structures*, vol. 83, n. 31-32, pp. 2513–2524, 2005.
[3] N. M. Newmark, "A method of computation for structural dynamics". *Journal of the engineering mechanics division*, vol. 85, n. 3, pp. 67-94, 1959.
[4] J. Chung and G. M. Hulbert, "A time integration algorithm for structural dynamics with improved numerical dissipation: the generalized-α method". *Journal of Applied Mechanics*, vol. 60, n. 2, pp. 371-375, 1993.
[5] J. Chung and G. M. Hulbert, "Explicit time integration algorithms for structural dynamics with optimal numerical dissipation", *Computer Methods in Applied Mechanics and Engineering*, vol. 137, n. 2, pp. 175-188, 1996.
[6] D. Soares and M. M. Rodrigues, "An optimized explicit-implicit time-marching formulation for dynamic analysis". *International Journal of Computational Methods*, vol. 18, n. 4, pp. 2050045, 2021.
[7] D. Soares, I. S. Sales, L. R. Pinto and W. J. Mansur, "A study on adaptive implicit-explicit and explicit-explicit time integration procedures for wave propagation analyses". *Acoustics*, vol. 6, n. 3, pp. 651-680, 2024.
[8] D. Soares, "A simple and effective new family of time marching procedures for dynamics". *Computer Methods in Applied Mechanics and Engineering*, vol. 283, pp. 1138-1166, 2015.
[9] D. Soares, "A model/solution-adaptive explicit-implicit time marching technique for wave propagation analyses". *International Journal for Numerical Methods in Engineering*, vol. 119, n. 7, pp. 590-617, 2019.
[10] D. Soares, "An enhanced explicit–implicit time-marching formulation based on fully-adaptive time-integration parameters". *Computer Methods in Applied Mechanics and Engineering*, vol. 403, pp. 115711, 2023.
[11] D. Soares, "An adaptive semi-explicit/explicit time marching technique for nonlinear dynamics". *Computer Methods in Applied Mechanics and Engineering*, vol. 354, pp. 637-662, 2019.
[12] J. Kennedy and R. Eberhart, "Particle swarm optimization". In: Proceedings of ICNN'95-international conference on neural networks, pp. 1942-1948.
[13] Y. Shi and R. Eberhart, "A modified particle swarm optimizer". In: 1998 IEEE international conference on evolutionary computation proceedings, *IEEE world congress on computational intelligence (Cat. No. 98TH8360)*, pp. 69-73.
[14] A. Gad, "Particle swarm optimization algorithm and its applications: a systematic review". *Archives of computational methods in engineering*, vol. 29, n. 5, pp. 2531-2561, 2022.
[15] O. C. Zienkiewicz and R. L. Taylor, *The Finite Element Method Vol. 1: The Basis*. Butterworth-Heinemann, 2000.
[16] R. C. Batra, M. Porfiri and D. Spinello, "Free and forced vibrations of a segmented bar by a meshless local Petrov–Galerkin (MLPG) formulation". *Computational Mechanics*, vol. 41, pp. 473-491, 2008.
[17] M. Fehler, "SEAM Update: SEAM phase I-RPSEA update: status of simulation". *The Leading Edge*, vol. 31, n. 12, pp. 1424-1426, 2012.